THE JOURNAL OF PHYSICAL CHEMISTRY A

Article

pubs.acs.org/JPCA

State-Dependent Global and Local Electrophilicity of the Aryl Cations

Sergey V. Bondarchuk*[,†] and Boris F. Minaev[†,‡]

[†]Department of Organic Chemistry, Bogdan Khmelnitsky Cherkasy National University, Boulevard Shevchenko 81, 18031 Cherkasy, Ukraine

[‡]Department of Chemistry, Tomsk State University, Prospekt Lenina 36, 634050 Tomsk, Russian Federation

Supporting Information

ABSTRACT: Two alternative approaches—vertical and adiabatic—are used to estimate global and local electrophilicity (ω and ω_k^+) indexes for a series of aryl cations in both the ground and first excited electronic states using the well-known Parr scheme. The energy parameters used in these methods are obtained by the B3LYP/6-311++G(2d,2p) calculations of the aryl cations and of their oxidized and reduced forms in acetonitrile medium. The ground state ω values are lower than those for the excited state, which is in accord with the maximum hardness principle. Analysis of the ω indexes calculated with more reliable adiabatic approach reveals a dependence of the ground and first excited state ω indexes on the singlet−triplet energy gap of the aryl cations. A plot of the above dependence has a hyperbola-like shape; thus, the maximum (ground state) and minimum (first excited state) ω indexes correspond to the aryl cation, for which the singlet−triplet splitting is close to zero. Moreover, the ω_k^+ index distribution at the ipso-carbon atoms does not obey the maximum hardness principle, since it depends on spin multiplicity, not on the electronic state spatial type. For many singlet ground state aryl cations, the ω_k^+ indexes at the ipso-carbon atom are lower when calculated in the excited triplet state; that is due to a strong ω delocalization onto two electrophilic centers. This explains a higher chemoselectivity of the triplet aryl cations in reactions with the π-nucleophiles compared to the corresponding singlet arylium species. Applicability of the adiabatic approach for calculation of the ω and ω_k^+ indexes is supported by the experimental data on the nucleophile-independent parameter E for the singlet and triplet state of the p-$Me_2NC_6H_4^+$ cation.

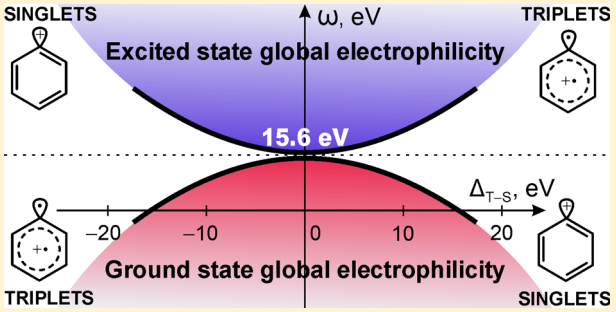

1. INTRODUCTION

Electrophilicity index (EI) is a simple, versatile, and clear chemical characteristic of an electron-deficient species.[1−5] This allows chemists to evaluate a priori the reactivity of an electrophilic molecule toward a nucleophilic (electron-rich) reagent. Today, many papers are published where calculations of the electrophilicity/nucleophilicity indexes for both neutral molecules and free radicals are presented.[6−8] A few reactivity indexes based on conceptual density functional theory[1−3,8−10] were developed to implement them in the study of organic reaction mechanisms involving electrophilic/nucleophilic reagents.[7,12−16] There are two most widely used types of the electrophilicity indexes.[1−16] The first of them—the global electrophilicity (ω) index—refers to general ability of a molecule to react with nucleophiles. The second type is the local electrophilicity (ω_k^+) index that preferably determines the active site of a molecule.[1−16] The global electrophilicity values ω can be calculated using the well-known Parr equation:[5]

$$\omega = \mu^2/2\eta \quad \text{(eV)} \tag{1}$$

where μ is the electronic chemical potential[17] and η is the chemical hardness.[18] These are usually defined in terms of the vertical ionization energy (IE) and electron affinity (EA) obtained on the basis of Koopmans' theorem as the following:[1−5]

$$\mu = -(\text{IE} + \text{EA})/2 \quad \text{(eV)} \tag{2}$$

$$\eta = \text{IE} - \text{EA} \quad \text{(eV)} \tag{3}$$

However, this method for estimation of the μ and η quantities provides rather inaccurate results for the ω value. This is connected with significant geometry changes during reduction and oxidation processes; the Franck−Condon factor therefore is rather small. Thus, the adiabatic approach to estimation of the IE and EA values provides much better results. As it follows from our present calculations, this change does significantly affect the final ω value. Therefore, the above method can be effectively used for the both closed-shell and ground state open-shell species, like free radicals.[6−8]

On the other hand, the ω value for excited high-spin molecules, like the aryl cations, cannot be estimated correctly in terms of the above simplified scheme. It is known that the aryl cations have close-lying singlet and triplet spin states depending of the substituents in the benzene ring;[19−22] electron donating

Received: February 18, 2014
Revised: April 4, 2014
Published: April 8, 2014

   dx.doi.org/10.1021/jp501740p | J. Phys. Chem. A 2014, 118, 3201−3210

substituents require the triplet ground state of the aryl cations, while electron withdrawing substituents cause the singlet ground state of the aryl derivatives. Parent phenyl cation has the ground singlet ($^1A_1$) state and the first excited triplet ($^3B_1$) state.[20,21,23] In contrast to the ortho-substituted aryl cations which undergo the intramolecular cyclization in the gas or liquid phase,[24,25] the photochemically generated para-substituted aryl cations effectively arylate a wide range of the π-electron donors yielding the corresponding arylation products.[26−28] This type of reaction has also been proposed for the "dark" conditions.[29,30]

It is known from the literature[31,32] that the arylating species in the above reactions are the triplet rather than the singlet aryl cations. They are less electrophilic and more selective than the singlet species. This is explained by the effective positive charge polarization, and shifting the electrophilic center toward the para-substituent that was found for the p-$NH_2C_6H_4^+$ cation.[33] Thus, estimation of the ω and ω_k^+ indexes for both the singlet and triplet state aryl cations is of current interest for both theoretical and practical points of view.

The first attempt to quantify the electrophile−nucleophile interactions was made by Swain and Scott.[34] Later on, this concept was extensively explored by Mayr et al.[35−49] This was resulted in development of an empirical equation (the Mayr−Patz equation), which was further modified by Albini et al.[50] for the aryl cations in the form

$$\log k = s(E + eN) \tag{4}$$

where N is the relative reactivity, E is the nucleophile-independent electrophilicity parameter, and s and e are the empirical parameters (e = 0.33 for the aryl cations).[50] According to this equation the E parameter was established for a wide range of various organic cations.[35−49] Pérez[51] has found that the E parameters for aryl diazonium cations are pretty well correlated (R = 0.9402) with the ω value calculated by the B3LYP/6-31G(d) approach in terms of vertical approximation. To the best of our knowledge, no data are present in the literature regarding calculations of the ω and ω_k^+ indexes for the aryl cations as well as for the high-spin molecules in general. Only for one cation (p-$NMe_2C_6H_4^+$) the E parameter was estimated.[50] On the other hand, the excited state electrophilicity for several diatomic molecules was calculated using the 4-31G basis set.[52] These calculations revealed the reliability of the maximum hardness principle.[53,54] Recently, this principle together with the minimum electrophilicity principle (MEP)[55] and the electrophilicity equalization principle (EEP)[56] has been actively debated.[57−59]

In this paper, we have calculated the ω and ω_k^+ indexes for a series of different ortho-, meta-, and para-substituted phenyl cations containing both the electron donating (EDG) and electron withdrawing (EWG) groups. The approach based on estimation of the μ and η values as the adiabatic differences between the corresponding oxidized, reduced, and initial forms of the molecule was found to be more reliable than the simplified vertical approach. The obtained theoretical results are useful for quantification of the relative reactivity of different spin states of the aryl cations toward different nucleophiles.

2. COMPUTATIONAL DETAILS

Geometry optimization of all studied species has been performed using the DFT[60]/B3LYP[61,62] method with Pople's split-valence triple-ζ basis set (6-311 G) and addition of both polarization (2d,2p) and diffuse (++) functions.[63] During geometry optimization no symmetry constraints have been used. Vibrational frequency analysis has been performed to evaluate the stationary points as a minimum (on a potential energy hypersurface). All the optimizations have been carried out using the polarizable continuum model (PCM)[64] in order to estimate the electrophilicity indexes of the studied systems under the liquid phase conditions. For this purpose we have chosen acetonitrile as being the most convenient solvent for experiments with the aryl cation reactivity.[25,27,28,31,32] To define cavities the universal force field (UFF) radii have been used. The overlap index and minimum radius of spheres have been specified as 0.8 and 0.5 Å, respectively. The DFT calculations of the closed-shell species have been performed using the spin-restricted Kohn−Sham formalism, while the open-shell species have been calculated in terms of the spin-unrestricted Kohn−Sham formalism. All geometry optimizations (the total number of stationary states is more than 150) have been performed with the Gaussian09 program package.[65]

Two approaches for estimation of the GE indexes, described in this paper, differ in methods for the calculation of ionization energy (IE) and electron affinity (EA) values. The more simplified vertical approach determines these quantities in terms of Koopmans' theorem as the following:

$$\mathrm{IE} = -E_{\mathrm{HOMO}} \quad \text{(eV)} \tag{5}$$

$$\mathrm{EA} = -E_{\mathrm{LUMO}} \quad \text{(eV)} \tag{6}$$

where HOMO and LUMO are the highest occupied and lowest unoccupied molecular orbitals of the given species. This approach has significant drawbacks due to high sensitivity of the basis set chosen. Expansion of the basis set and/or addition of the diffuse function dramatically decreases the accuracy. Additional virtual orbitals affect significantly the relative position of the LUMO and, as a result, the final EA value.[66] It was empirically found that the most appropriate basis set is 6-31G(d).[1−16] Thus, calculations of the IE and EA in terms of the vertical approach need some compromise between relatively low accuracy during geometry optimization and more or less satisfactory prediction of the EA value.

This significant drawback is almost completely removed in the adiabatic approach, which defines the IE and EA values as the following:

$$\mathrm{IE} = U^{\mathrm{RD}} - U^{\mathrm{C}} = (E_{\mathrm{elec}}^{\mathrm{RD}} + \mathrm{ZPVE}^{\mathrm{RD}}) - (E_{\mathrm{elec}}^{\mathrm{C}} + \mathrm{ZPVE}^{\mathrm{C}}) \tag{7}$$

$$\mathrm{EA} = U^{\mathrm{C}} - U^{\mathrm{R}} = (E_{\mathrm{elec}}^{\mathrm{C}} + \mathrm{ZPVE}^{\mathrm{C}}) - (E_{\mathrm{elec}}^{\mathrm{R}} + \mathrm{ZPVE}^{\mathrm{R}}) \tag{8}$$

where U^{RD}, U^{C}, and U^{R} are the total energies of the oxidized radical dicationic, starting cationic (singlet or triplet), and reduced radical state of the molecule at 0 K, respectively (Scheme 1). These are the sums of the corresponding energies for the stationary points on the Born−Oppenheimer potential energy surfaces (E_{elec}) and zero-point vibration energy (ZPVE).

Since the global electrophilicity of a molecule is distributed following the electrophilic Fukui function on atoms, one can write[51]

$$\omega_k^+ = f_k^+ \omega \tag{9}$$

where ω_k^+ is the local electrophilicity index condensed to site k in the molecule and the f_k^+ is the electrophilic Fukui function (i.e., the Fukui function for a nucleophilic attack).[67] The f_k^+ values were calculated using the DMol3 module[68,69]

Scheme 1. Species Used for Calculations of the Ionization Energy and Electron Affinity of the Aryl Cations in Terms of the Adiabatic Approach

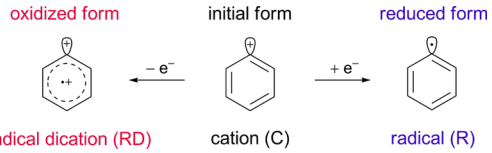

implemented in Materials Studio 5.5 suite of the programs.[70] The BLYP functional[62,71] and the triple-numerical polarization basis set, namely, TNP,[68,69] was used during the calculations. This basis set has been chosen because its effectiveness is superior to that of a comparable in size Gaussian basis set (namely, triple-ζ plus double polarization functions) in terms of accuracy per computational cost.[72] The polar medium simulation was performed using a conductor-like screening model (COSMO).[73,74] Computation of the f_k^+ values was carried out using the atomic charges determined by the post-SCF Hirshfeld population analysis.[75] The Hirshfeld atomic charges were favored because of their little dependence on the basis set used.[76−78]

3. RESULTS AND DISCUSSION

3.1. Effect of the Basis Set Expansion in Prediction of the IE and EA Values in Terms of the Vertical and Adiabatic Approximations. To find out the most appropriate method for estimation of the ω indexes, we have performed calculations of the latter quantities for methyl (MR), vinyl (VR), and phenyl (PR) radicals. These compounds have been chosen because their experimental IE and EA are known[79] and the ω indexes have been recently calculated in terms of the vertical approach.[6] The aim of these calculations was to determine how the basis set expansion affects the resulting IE and, especially, EA values. The results are presented in Tables S1−S2 in the Supporting Information. The experimental IE and EA values are equal to 9.84 vs 8.25 and 0.00 vs 0.67 eV for the MR and VR, respectively.[79] Thus, the final ω indexes for these radicals are equal to 1.23 and 1.31 eV, respectively (Table S1 in the Supporting Information). Domingo et al.[6] calculated the latter indexes in terms of the vertical approach using the B3LYP/6-31G(d) method. The obtained values are equal to 1.43 and 1.84 for the MR and VR, respectively.[6]

As one can see in Table S1 in the Supporting Information, the IE and EA values calculated in terms of the vertical approach provide generally poor coincidences with experiment. The maximum deviations $|\Delta(\mathrm{IE})|_{max}$ and $|\Delta(\mathrm{EA})|_{max}$ for the MR are equal to 3.78 eV for the 3-21G basis set and 2.19 eV for the 6-311++G(2d,2p) and 6-311++G(3df,3pd) basis sets (Table S2 in the Supporting Information). Meanwhile, the same results corresponding to the VR are slightly better; the $|\Delta(\mathrm{IE})|_{max}$ and $|\Delta(\mathrm{EA})|_{max}$ are equal to 1.96 (6-31G basis set) and 1.71 eV (6-311+G(d,p), 6-311++G(2d,2p), and 6-311++G(3df,3pd) basis sets), respectively (Table S1 in the Supporting Information). It is clear that the small basis provides better EA energies but poorer IE energies and vice versa. Furthermore, it is a known fact that expansion of the basis set does change the EA values more strongly.[66] Also addition of the diffuse functions results in dramatic increasing of the $|\Delta(\mathrm{EA})|_{max}$ values (Table S2 in the Supporting Information).

For the vertical approach, the final ω indexes, which have been found to be the closest to the experimental ones, corresponded to the 3-21G basis set (Table S1 in the Supporting Information). The $\delta(\omega)$ values for the MR and VR have been found to be 11.60 and 26.85%, respectively (Table S2 in the Supporting Information). Thus, one can conclude that using the vertical approach needs a compromise between relatively poor basis set quality during geometry optimization and satisfactory values of the IE and EA quantities. Finally, the "standard" basis set 6-31G(d), which is generally accepted for such calculations,[6−8,14,47] provides rather poor results for the MR and VR; the $\delta(\omega)$ is equal to 13.82 and 28.20%, respectively (Table S2 in the Supporting Information).

On the other hand, the adiabatic approach provides much more accurate performance in prediction the IE and EA quantities (Table S1 in the Supporting Information). The maximum deviations $|\Delta(\mathrm{IE})|_{max}$ and $|\Delta(\mathrm{EA})|_{max}$ for the MR and VR are equal to 0.11 vs 0.42 and 0.09 vs 1.14 eV, respectively. Generally, when moving from the 3-21G to 6-311++G-(3df,3pd) basis set, the results become more accurate for the EA values (Tables S1 and S2 in the Supporting Information). In contrast, the $|\Delta(\mathrm{IE})|_{max}$ increases a little when the basis set extension occurs (Tables S2 in the Supporting Information). Nevertheless, this increasing is not enough to change noticeably the final ω index. Therefore, we decided to use the 6-311++G(2d,2p) basis set in the present study as a minimum required for accurate enough prediction of the ω indexes. The latter indexes for the MR and VR calculated using the 6-311++G(2d,2p) basis set in terms of the adiabatic approach are equal to 1.21 and 1.37 versus 1.23 and 1.31 computed using the experimental IE and EA values (Table S1 in the Supporting Information). The $\delta(\omega)$ for the MR and VR are much less than that for the vertical approach and equal to 1.57 and 4.41%, respectively.

3.2. Global Electrophilicity ω Indexes for the Series of 25 Aryl Cations in Their Singlet and Triplet Spin States. The aryl cations which were selected for the present study are illustrated in Chart 1. The selection criteria were the following: (a) appearance of the cations in the experimentally known reactions[25−28,31,32,50] (the cations **1**, **4**, **6**, **8**, **9**, **15**, **18**, **19**, **24**); (b) ability for comparison of the ω indexes with that for the aryl diazonium cations[45] being a potential aryl cation precursor (the cations **10**, **12**, **13**, **14**, **16**, **20**, **21**, **22**, **23**, **25**); (c) ability for determination of the ortho-, meta-, and para-substituents' influence on the ω values as well as the effect of multiple substitution in the case of both electron releasing (NH_2 and OCH_3) and electron withdrawing (Cl) groups (the rest of the cations **2**, **3**, **5**, **7**, **11**, and **17**).

Let us first consider the influence of the substituents on the triplet−singlet energy splitting (Δ_{T-S}). In Chart 1 the aryl cations are sorted in the order of the Δ_{T-S} value increase; these quantities are listed in Table 1. Herein, the most interesting observation is that all the substituents possessing the positive inductive and resonance effects, except the CN group, decrease the Δ_{T-S} value compared to the parent phenyl cation **21** (Table 1). For the cyano derivative **20** the Δ_{T-S} value is less than 0.9 kcal mol^{-1} (Table 1). The strong electron withdrawing groups (NO_2, $COOCH_3$, CF_3) possessing negative inductive and resonance effects increase the Δ_{T-S} value up to 2.6 kcal mol^{-1} (Table 1).

The second observation is that the inductive effect of a substituent plays a minor role in changing the Δ_{T-S} value compared to the resonance effect. Thus, for the alkyl derivatives **15**, **16**, **18**, and **19** the Δ_{T-S} energy decrease is less than for the bromo and chloro derivatives (**13** and **14**) providing negative

dx.doi.org/10.1021/jp501740p | J. Phys. Chem. A 2014, 118, 3201−3210

Chart 1. Aryl Cations Selected for Study in This Work[a]

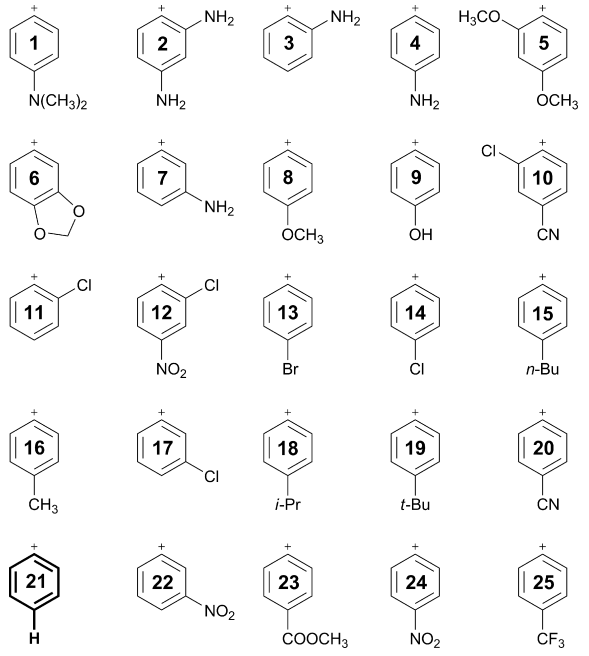

[a]Numeration corresponds to increasing the ΔE_{T-S} value. The cations **1**–**7** have the triplet ground state, and the species **9**–**25** have the singlet state. The cation **8** has the ΔE_{T-S} value being close to zero.

inductive, but positive resonance effect (deactivating groups). Moreover, the doubly substituted cations **10** and **12** provide the Δ_{T-S} energy being equal to ca. 7–8 kcal mol^{-1} (Table 1); that is less than for each cation individually. Thus, one can talk about the antagonistic effect of the multiple electron withdrawing substituents. In contrast, the electron releasing groups provide an additive effect leading to larger decrease of the Δ_{T-S} value (Table 1).

The third observation concerns the ortho-, meta-, and para-substitution effect. As it can be seen in Table 1, in order of decreasing Δ_{T-S} energy, the substituents are placed as the following: the ortho, para, and meta derivatives. This effect occurs in the case of both the electron releasing (NH_2) and withdrawing (Cl) groups (Table 1).

Finally, the Δ_{T-S} energies found in this work are in accord with the previous studies.[19−22] The only difference is that we have found the cation **8** as being isoenergetic in both the singlet and triplet electronic states, while according to the previous B3LYP/6-31G(d)[19−21] and B3LYP/6-311+G(d)[22] calculations, this is a quasidegeneracy characteristic for the OH derivative (**9**).

Based on the results obtained for the MR and VR species we have calculated the IE and EA values for the PR by means of the above two approaches. The experimental IE and EA energies for this radical are equal to 8.32 and 1.10 eV, respectively.[79] Meanwhile, the calculated ones are found to be 8.24 and 1.07 eV (the 6-311++G(2d,2p) basis set) for adiabatic approach and 6.47 and 2.01 eV (the 6-31G(d) basis set) for vertical approach. Taking into account the above quantities the

Table 1. DFT Parameters, Namely, the Triplet−Singlet Adiabatic Energy Difference (Δ_{T-S}) in kcal mol^{-1}, Electronic Chemical Potential (μ), Chemical Hardness (η), and Global Electrophilicity Indexes Obtained with the Vertical ω_{vert} and Adiabatic ω_{adiab} Approaches in eV for the Series of the Aryl Cations

		singlet state cations							triplet state cations						
			adiabatic approach			vertical approach				adiabatic approach			vertical approach		
cation	Δ_{T-S}	state	μ	η	ω_{adiab}	μ	η	ω_{vert}	state	μ	η	ω_{adiab}	μ	η	ω_{vert}
1	−13.7	$\tilde{A}^1A'$	−6.23	0.91	21.26	−5.89	2.15	8.06	$\tilde{X}^3A$	−6.23	2.10	9.25	−6.20	2.52	7.64
2	−12.6	$\tilde{A}^1A$	−6.12	0.82	22.90	−5.97	2.49	7.17	$\tilde{X}^3A'$	−6.12	1.91	9.78	−5.91	2.23	7.82
3	−10.7	$\tilde{A}^1A$	−6.65	1.15	19.14	−6.31	2.38	8.36	$\tilde{X}^3A''$	−6.65	2.08	10.60	−6.59	2.46	8.80
4	−10.2	$\tilde{A}^1A'$	−6.44	1.00	20.86	−6.12	2.33	8.03	$\tilde{X}^3B_1$	−6.44	1.88	11.04	−6.51	2.52	8.40
5	−9.6	$\tilde{A}^1A$	−6.89	1.20	19.76	−6.53	2.65	8.05	$\tilde{X}^3A''$	−6.89	2.03	11.68	−6.78	2.38	9.67
6	−7.7	$\tilde{A}^1A$	−6.76	1.17	19.60	−6.36	2.57	7.89	$\tilde{X}^3A''$	−6.76	1.83	12.47	−6.73	2.22	10.19
7	−1.9	$\tilde{A}^1A$	−6.49	1.46	14.49	−6.09	2.96	6.28	$\tilde{X}^3A''$	−6.49	1.62	13.03	−6.61	2.32	9.42
8	0.0	$^1A'$	−6.88	1.52	15.56	−6.51	2.55	8.30	$^3A''$	−6.88	1.52	15.58	−7.10	2.46	10.25
9	2.1	$\tilde{X}^1A'$	−7.05	1.74	14.23	−6.66	2.74	8.09	$\tilde{A}^3A''$	−7.05	1.56	15.91	−7.30	2.53	10.54
10	7.2	$\tilde{X}^1A'$	−7.91	1.83	17.13	−7.55	2.90	9.84	$\tilde{A}^3A''$	−7.91	1.20	26.04	−8.16	2.06	16.21
11	7.5	$\tilde{X}^1A'$	−7.53	1.87	15.19	−7.17	2.93	8.77	$\tilde{A}^3A''$	−7.53	1.21	23.38	−7.86	2.24	13.79
12	7.7	$\tilde{X}^1A'$	−8.00	1.83	17.47	−7.63	2.92	9.96	$\tilde{A}^3A''$	−8.00	1.16	27.59	−8.32	2.16	16.05
13	10.3	$\tilde{X}^1A_1$	−7.26	1.84	14.34	−6.84	2.77	8.44	$\tilde{A}^3B_1$	−7.26	0.95	27.85	−7.65	2.08	14.03
14	11.2	$\tilde{X}^1A_1$	−7.38	2.04	13.33	−6.99	3.04	8.02	$\tilde{A}^3B_1$	−7.38	1.07	25.35	−7.72	2.18	13.70
15	12.8	$\tilde{X}^1A'$	−7.01	1.98	12.45	−6.80	3.34	6.92	$\tilde{A}^3A'$	−7.01	0.86	28.55	−7.44	2.19	12.65
16	13.3	$\tilde{X}^1A'$	−7.18	2.30	11.22	−6.87	3.48	6.79	$\tilde{A}^3A'$	−7.18	1.15	22.46	−7.54	2.24	12.69
17	13.7	$\tilde{X}^1A'$	−7.39	2.07	13.21	−7.03	3.08	8.01	$\tilde{A}^3A''$	−7.39	0.88	31.00	−7.69	1.84	16.03
18	13.8	$\tilde{X}^1A'$	−7.09	2.13	11.77	−6.85	3.46	6.78	$\tilde{A}^3A$	−7.09	0.93	26.88	−7.48	2.20	12.71
19	13.9	$\tilde{X}^1A'$	−7.04	2.07	11.99	−6.82	3.45	6.74	$\tilde{A}^3A''$	−7.04	0.86	28.88	−7.51	2.19	12.89
20	19.8	$\tilde{X}^1A_1$	−7.79	2.53	11.98	−7.43	3.57	7.75	$\tilde{A}^3B_1$	−7.79	0.81	37.45	−8.19	1.85	18.07
21	20.7	$\tilde{X}^1A_1$	−7.46	2.75	10.11	−7.13	3.84	6.62	$\tilde{A}^3B_1$	−7.46	0.96	29.11	−7.86	2.05	15.09
22	20.9	$\tilde{X}^1A'$	−7.94	2.58	12.20	−7.69	3.77	7.84	$\tilde{A}^3A''$	−7.94	0.77	41.12	−8.36	1.91	18.31
23	21.0	$\tilde{X}^1A'$	−7.54	2.47	11.52	−7.08	3.37	7.45	$\tilde{A}^3A''$	−7.54	0.65	43.97	−7.86	1.87	16.51
24	22.6	$\tilde{X}^1A_1$	−7.91	2.56	12.20	−7.57	3.68	7.79	$\tilde{A}^3B$	−7.91	0.61	51.54	−8.28	1.88	18.23
25	23.3	$\tilde{X}^1A'$	−7.84	2.80	10.97	−7.50	3.88	7.25	$\tilde{A}^3A''$	−7.84	0.78	39.59	−8.27	1.94	17.62

dx.doi.org/10.1021/jp501740p | J. Phys. Chem. A 2014, 118, 3201−3210

resulting ω indexes should be the following: 1.54 (experiment), 1.51 (adiabatic), and 2.02 eV (vertical).[6] No doubt that the above discussion exhaustively suggests the advantages of the adiabatic approach over the vertical one. It should be stressed that the ω indexes obtained within these two different methods are not comparable with each other. Thus, we will not discuss the relative place of the aryl cations' ω indexes in the previously developed global electrophilicity scale.[6,80]

The ω_{vert} indexes vary slightly (Table 1) from 6.28 eV for the $\tilde{A}^1A$ cation **7** and 7.64 eV for the $\tilde{X}^3A$ cation **1** up to 9.96 eV for the $\tilde{X}^1A'$ cation **12** and 18.31 eV for the $\tilde{A}^3A''$ cation **22**. In contrast, the ω_{adiab} indexes vary very widely (Table 1) from 10.11 eV for the $\tilde{X}^1A_1$ parent cation **21** and 9.25 eV for the $\tilde{X}^3A$ cation **1** up to 22.90 eV for the $\tilde{A}^1A$ cation **2** and 51.54 eV for the $\tilde{A}^3B$ cation **24**. According to the experimental results on the nucleophile-independent parameter E for the singlet and triplet state p-$Me_2NC_6H_4^+$ cation (**4**) obtained by Albini et al.[50] using eq 4 the E value for the triplet cation was found to be 8.11, while for the singlet species this was found to be higher than 20. As one can see in Table 1, the vertical approach completely failed (the ω_{vert} values for the triplet and singlet are equal to 8.03 and 8.40 eV, respectively) in prediction of the global electrophilicity of this cation. On the other hand, the calculated data obtained by the adiabatic approach provided more realistic results (the ω_{adiab} are equal to 11.04 eV for the triplet cation and 20.86 eV for the singlet cation).

It is scarcely possible to foresee whether the ω_{vert} value for the triplet $\tilde{X}^3B_1$ cation (**4**) is randomly closer to the experimental one than the ω_{adiab} (Table 1), but in the case of the singlet $\tilde{A}^1A'$ cation the latter value is incomparably closer than the ω_{vert}. Unfortunately, we could not find in the literature the data concerning the E parameter for the other cations, but taking into account the above discussion we believe that the ω_{adiab} indexes are more reliable. Thus, the further discussion of the global and local electrophilicity indexes will concern only the results obtained by the adiabatic approach, while the ones for the vertical approximation are present in the Supporting Information. It also should be note that the vertical approach can be effectively used to predict the ω indexes for those ground state species which have well-separated ground and first excited electronic states, e.g., the ω indexes for aryl diazonium cations correlate well with the experimental E parameters.[51]

As one can see in Figure 1a, the ω_{adiab} indexes well correlate with the triplet−singlet energy splitting (Δ_{T-S}) for the aryl cations. The singlet state ω_{adiab} decreases with rise of the Δ_{T-S} difference, while the triplet state values behave vice versa. Besides, if one sorts the ω_{adiab} indexes separately for the ground and first excited electronic states, they arrange themselves like a hyperbola (Figure 1a). Thus, one can conclude that the ground state global electrophilicity increases and the first excited state global electrophilicity decreases when the triplet−singlet energy splitting goes to zero.

On the grounds of the E parameters and ω_{adiab} indexes for the cation **4**, the aryl cations can be estimated as very strong electrophiles (Table 1) and, in overall cases, these should be placed far beyond the multichlorinated benzhydryl cations (E = 10−14) in the well-known benzhydrylium electrophilicity scale.[35−49,82,83] It was shown[50] that the singlet state cation **4** reacts at the diffusion-controlled rate ($k \cong 1.2 \times 10^{10}$ M^{-1} s^{-1}) even with weak nucleophiles with no selectivity. In contrast the triplet state cation **4** reacts at the measurable rates ($\log {}^3k_{NuH}/s \cong 6-12$) with several alkenes and alkynes.[50] Thus, all the excited state cations **1**−**25** as well as the ground state cations

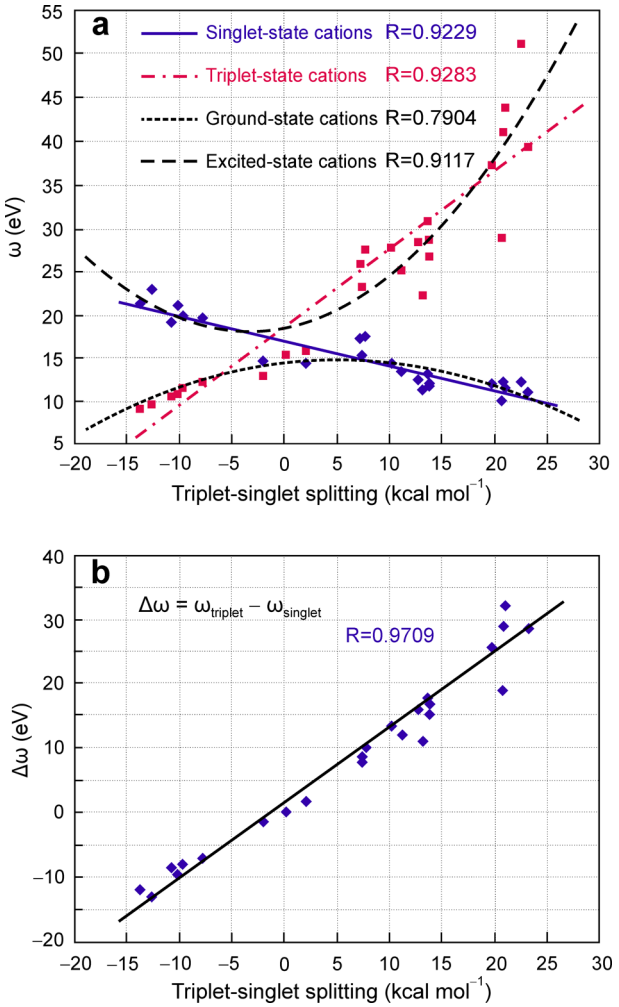

Figure 1. Plot of the global electrophilicity ω index (a) and the difference between the triplet and singlet ω indices (b) versus the triplet−singlet energy splitting Δ_{T-S} of the series of the aryl cations studied.

8−**13** are expected to react at the diffusion-controlled rate with typical π-nucleophiles, since their ω_{adiab} indexes are noticeably higher than that of the cation **4** ($\tilde{X}^3B_1$). Only the cations **1** ($\tilde{X}^3A$), **2** ($\tilde{X}^3A'$), and **3** ($\tilde{X}^3A''$) should react at the lower rate; the ω_{adiab} are equal to 9.25, 9.78, and 10.60 eV, respectively (Table 1).

It should be noted that a boundary between the ground and excited state electrophilicity lies at 15.6 eV as it follows from our present PCM/B3LYP/6-311++G(2d,2p) calculations. This is peculiar for cation **8**, since this has two quasi-isoenergetic spin states ($^1A'$ and $^3A''$). In order to obtain a simple and clear correlation combining the ω indexes and the Δ_{T-S} energies, we have built the plot (Figure 1b). This displays a rather good correlation (R = 0.97).

3.3. Local Electrophilicity ω^+ Indexes for the Singlet and Triplet Spin State Aryl Cations. The local electrophilicity index condensed to molecular site k (ω_k^+) is a simple descriptor which allows one to study regio- and/or chemoselectivity in organic reactions.[6] In contrast to recently studied captodative free radicals,[6] when reacting with π-nucleophiles, the aryl cations *always* behave as electrophiles. Additionally, similar to aryl diazonium cations for which the two potential local reactivity centers (the α and β nitrogen atoms) are

dx.doi.org/10.1021/jp501740p | J. Phys. Chem. A 2014, 118, 3201−3210

present,[51] the aryl cations have two most electrophilic centers. The electrophilic Fukui function distribution in the singlet and triplet cation **4** is plotted in Figure 2.

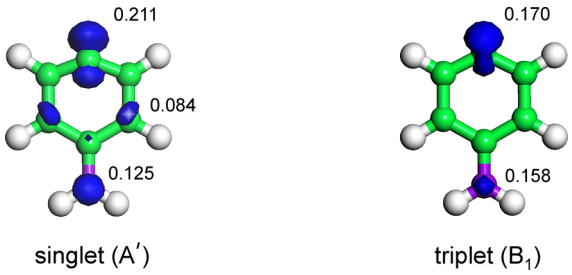

Figure 2. The main contribution of the electrophilic Fukui function (f^+) in the singlet and triplet cation **4** calculated using the Hirshfeld atomic charges by DMol3 program.

The major contribution of the f^+ function is on the ipso-carbon atoms. A significant, but somewhat smaller, part of the f^+ is located on the nitrogen atom. While for the $\tilde{X}^3B_1$ cation **4** the f^+_{ipso}: f^+_N ratio is close to 1:1, the same ratio for the $\tilde{A}^1A'$ cation **4** is about 2:1 (Figure 2). Note that these ratios remain for the rest of the cations, for which the second largest contribution is localized on the other ring or substituent atom. The ratio between the singlet $f^+_{ipso}(S)$ and triplet $f^+_{ipso}(T)$ local electrophilicity Fukui functions on the ipso-carbon atom (Table 2) is about 2:1. Meanwhile, the local electrophilicity indexes $\omega^+_{ipso}(S)$ and $\omega^+_{ipso}(T)$ do not obey this ratio because of significant deviation in the ω_{adiab} indexes on which the local electrophilicity indexes are calculated eq 9.

Table 2. Local Reactivity Indexes at the Ipso-Carbon Atom for the Series of the Singlet and Triplet Aryl Cations 1−25 Calculated in Terms of the Adiabatic Approach[a]

cation	$f^+_{ipso}(S)$	$f^+_{ipso}(T)$	$Q^{(S)}_{ipso}$	$Q^{(T)}_{ipso}$	$\omega^+_{ipso}(S)$	$\omega^+_{ipso}(T)$
1	0.196	0.144	0.089	0.046	4.17	1.33
2	0.197	0.142	0.022	0.051	4.51	1.39
3	0.188	0.124	0.153	0.049	3.60	1.31
4	0.211	0.170	0.123	0.069	4.40	1.88
5	0.186	0.142	0.095	0.081	3.68	1.66
6	0.193	0.133	0.122	0.072	3.78	1.66
7	0.197	0.156	0.114	0.071	2.85	2.03
8	0.225	0.197	0.222	0.108	3.50	3.07
9	0.247	0.208	0.229	0.122	3.51	3.31
10	0.244	0.139	0.258	0.141	4.18	3.62
11	0.249	0.149	0.232	0.115	3.78	3.48
12	0.230	0.116	0.263	0.133	4.02	3.20
13	0.236	0.177	0.241	0.155	3.38	4.93
14	0.269	0.185	0.248	0.168	3.59	4.69
15	0.278	0.172	0.230	0.150	3.46	4.91
16	0.283	0.188	0.231	0.166	3.18	4.22
17	0.258	0.165	0.241	0.195	3.41	5.12
18	0.280	0.180	0.229	0.160	3.30	4.84
19	0.281	0.176	0.229	0.162	3.37	5.08
20	0.284	0.196	0.267	0.274	3.40	7.34
21	0.286	0.225	0.237	0.253	2.89	6.55
22	0.264	0.184	0.257	0.264	3.22	7.57
23	0.265	0.178	0.253	0.196	3.05	7.83
24	0.276	0.182	0.274	0.224	3.37	9.38
25	0.291	0.223	0.261	0.282	3.19	8.83

[a]Electrophilic Fukui functions $f^+_{ipso}(S)$ and $f^+_{ipso}(T)$, charge partitioning by Hirshfeld method $Q^{(S)}_{ipso}$ and $Q^{(T)}_{ipso}$, and the local electrophilicity $\omega^+_{ipso}(S)$ and $\omega^+_{ipso}(T)$ indexes in eV.

As one can see in Table 2, the $\omega^+_{ipso}(T)$ indexes for the cations **1−12** are less than the corresponding $\omega^+_{ipso}(S)$ values. This characterizes the latter cations as less electrophilic and more chemoselective than the singlet ones. Thus, the $\tilde{X}^3B_1$ cation **4** selectively arylates π-nucleophiles (e.g., 1-hexene) according to Markovnikov regioselectivity, while the $\tilde{A}^1A'$ cation **4** is electrophilic enough to react unselectively with whole double bond to form a cationic spiroadduct.[84] Hence, there is a dependence between the chemoselectivity and the local electrophilicity of the aryl cations. Similar to the ω_{adiab} indexes, the ω^+_{ipso} values depend predominantly on the Δ_{T-S} energy rather than on the nature of the substituent in the benzene nucleus. Figure 3 represents the correlation between

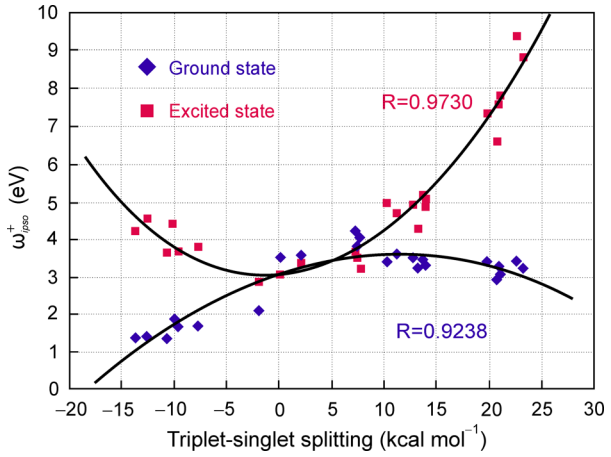

Figure 3. Plot of the local electrophilicity index ω^+_{ipso} at the ipso-carbon atom versus the triplet−singlet energy splitting Δ_{T-S} of the series of aryl cations studied.

the ground and first excited state local ω^+_{ipso} values and the Δ_{T-S} energy. With correction by the f^+_{ipso} functions, the ω^+_{ipso} indexes provide somewhat higher regression coefficients compared to that of the ω_{adiab} indexes (Figure 1a). In contrast to the ω_{adiab}, the ground state local electrophilicities of the cations for which the Δ_{T-S} difference is positive are significantly higher ($\omega^+_{ipso} \cong$ 1−3 eV) than those with the $\Delta_{T-S} < 0$ ($\omega^+_{ipso} \cong$ 3−4 eV) (Figure 3).

Important information about the local reactivity of the cations **1−25** can be derived using Morell's dual operator $\Delta f(\vec{r})$.[85] The corresponding index is written as the difference between nucleophilic and electrophilic Fukui functions, thus being able to characterize both reactive behaviors. It is shown[86] that the new descriptor correctly predicts the site reactivity induced by different donor and acceptor groups in substituted phenyl molecules. If $\Delta f(\vec{r}) > 0$, then the site is favored for a nucleophilic attack, whereas if $\Delta f(\vec{r}) < 0$, then it may be favored for an electrophilic attack. Recently, Morell's dual operator was extended to excited states.[86,87] It was proven that the ground state $\Delta f_0(\vec{r})$ and the first excited state $\Delta f_1(\vec{r})$ operators have the same form:[86,87]

$$\Delta f_0(\vec{r}) \cong \Delta f_1(\vec{r}) \cong \rho_{LUMO}(\vec{r}) - \rho_{HOMO}(\vec{r}) \cong f^+(\vec{r}) - f^-(\vec{r}) \quad (10)$$

dx.doi.org/10.1021/jp501740p | J. Phys. Chem. A 2014, 118, 3201−3210

Herein, $\rho_{HOMO}(\vec{r})$ and $\rho_{LUMO}(\vec{r})$ are the electronic density; $f^{-}(\vec{r})$ is the nucleophilic Fukui function; subscripts 0 and 1 denote the ground and first excited states.

We have calculated Morell's dual operator for the cations **1**−**25**; the results are collected in Table S5 in the Supporting Information. We have denoted the singlet and triplet indexes as $\Delta f_S(\vec{r})$ and $\Delta f_T(\vec{r})$, respectively. The obtained results suggest that the singlet state cations have the electrophilic nature at the ipso-carbon ($\Delta f(\vec{r}) > 0$). In contrast, the triplet cations look like the radicaloid species (Table S5 in the Supporting Information), which supports the previous conclusions about the nature of the triplet state cations.[23−34] The $\Delta f_T(\vec{r})$ values are very close to zero and even slightly negative, but it should be noted that the electrophilic character somewhat increases with the rise of the Δ_{T-S} energy for the both singlet and triplet cations. Thus, Morell's dual operator can help to rationalize the difference in chemical reactivity of the singlet and triplet aryl cations.[26−28]

3.4. Structural Performance and Electrophilicity Indexes for the Singlet State 2,4,6-Triamino- and 2,4,6-Trimethoxyphenyl Cations. Quite unexpected results were obtained after the geometry optimization of the 2,4,6-triamino- (**26**) and 2,4,6-trimethoxyphenyl (**27**) cations. These were found to be absolutely unstable in the form of the aryl cations; as a result, a breaking of the benzene nuclei occurred followed by an intramolecular rearrangement. The optimized bicyclic cationic structures are illustrated in Figure 4. This

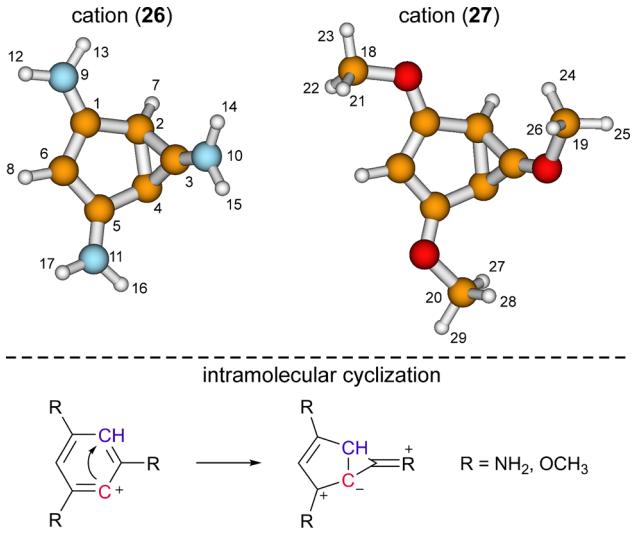

Figure 4. The structures obtained after geometry optimization of the 2,4,6-triamino- (**26**) and 2,4,6-trimethoxyphenyl (**27**) cations in their singlet state with B3LYP/6-311++G(2d,2p) method in MeCN (top); geometry transformation leading to the cyclic cations in their plausible resonance structures (bottom).

process is similar to the previously found cyclization that is peculiar for a number of the ortho-substituted aryl cations.[24] It is known[19−22] that electron donating substituents destabilize the singlet state of the aryl cations (e.g., the $\tilde{A}^1A'$ cation **4** has the ipso-carbon atom lying out of the plane). Thus, the singlet cations **1**−**7** have nonplanar benzenoid rings and completely broken aromatic system. Being a high electrophilic center the ipso-carbon atom in the cations **26** and **27** captures the meta-carbon atom to form the covalent bond $C(4)_{ipso}-C(2)_{meta}$ (Figure 4). On the basis of the electrophilic Fukui function (f^+) distribution and the molecular electrostatic potential maps (Figure 5), we assume that the most plausible resonance structures for the cations **26** and **27** are those illustrated in Figure 4 (bottom).

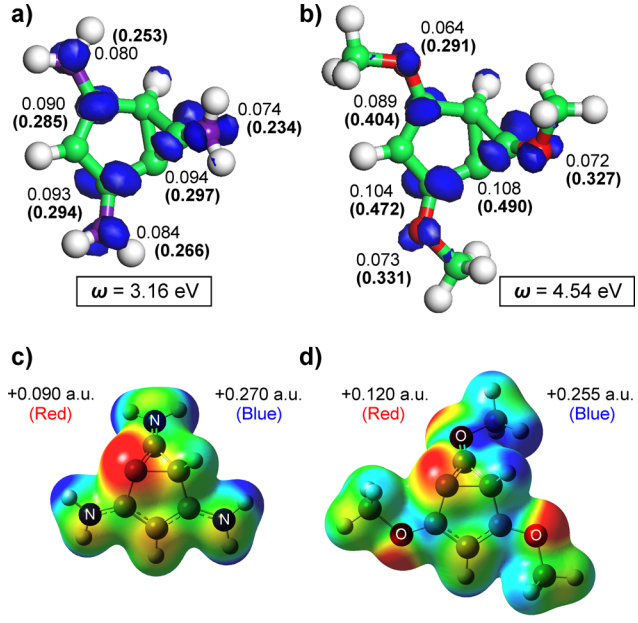

Figure 5. The main contribution of the electrophilic Fukui function (f^+) and the corresponding ω^+ values (in parentheses) for the cations **26** (a) and **27** (b); molecular electrostatic potential maps for the cations **26** (c) and **27** (d) built by the GaussView 3.07 program.

Another interesting feature of the cations **26** and **27** is extremely low global electrophilicity (Figure 5). Their ω_{adiab} indexes are 3- to 5-fold lower than the typical ones for the singlet cations **1**−**7** (Table 1). Moreover, the global electrophilicity is almost equally spread all over the cations **26** and **27**, which follows from the electrophilic Fukui function (f^+) distribution (Figure 5). There is no explicit most electrophilic center in the bicyclic cations which can accept an anion. We have tried to optimize structures with the chloride anion attached to each electrophilic center (Figure 5), but these calculations have failed (i.e., the chloride anions moved away up to 5 Å). The reason for such unusual behavior is a strong positive charge delocalization resulting in dramatically low electrophilicity (Figure 5). Molecular electrostatic potential maps (Figure 5) revealed that former ipso-carbon atom C(4) has the lowest value of the potential in the cations **26** (+0.090) and **27** (+0.120). Therefore, the second possible way for stabilization of these cations is deprotonation,[24] but this is the issue of further study.

To gain additional information about the cations **26** and **27** we have calculated the ring strain energy (RSE) for the three-membered (**A**) and five-membered (**B**) cycles. Calculations are based on the use of the empirical regression equation recently obtained by Frontera et al.[88] for unsaturated cycles:

$$RSE = 337.72 \times G(r) - 8.115 \quad (kcal\,mol^{-1}) \qquad (11)$$

Herein, $G(r)$ is the kinetic energy density (in au) in the corresponding ring critical point (RCP) obtained by means of the Bader's theory of "atoms in molecules".[89,90] This is a simple and convenient method of RSE estimation that is free from other influences, as the number and type of reference molecules

dx.doi.org/10.1021/jp501740p | J. Phys. Chem. A 2014, 118, 3201−3210

and type of reaction (isodesmic, homodesmotic, hyper-homodesmotic, etc.).[88] The obtained RSE values are listed in Table 3.

Table 3. Ring Strain Energies, RSE (kcal mol^{-1}), and Kinetic Energy Density in the Corresponding Ring Critical Points (au) for the Cations 26 and 27

ring	RSE	$G(r)$	ring	RSE	$G(r)$
26A	48.8	0.1686	26B	14.2	0.0661
27A	48.8	0.1686	27B	14.3	0.0665

As one can see in Table 3, the RSE values for the rings **A** are rather high (48.8 kcal mol^{-1}); these are close to those of cyclopropanone and 2,2-dimethylcyclopropanone (46.1 and 45.1 kcal mol^{-1}, respectively).[88] On the other hand, the RSE values for cyclopropene and 1-methyl-1-cyclopropene (54.5 kcal mol^{-1}) as well as for 1,2-dimethyl-1-cyclopropene (51.5 kcal mol^{-1}) are even higher than those calculated for the cycles **A**. Thus, we can assume that the cations **26** and **27** are stable enough to exist under the liquid phase conditions.

Furthermore, the rings **B** are more strained than typical 5-membered cycles. The calculated RSE values are about twice as high as those of cyclopentane and cyclopentene (7.4 and 6.8 kcal mol^{-1}, respectively).[88] Meanwhile, the rings **B** do not break after both single-electron oxidation and reduction of the cations **26** and **27** (the optimized structures are presented in the Supporting Information). In contrast, the rings **A** were found to be unstable with respect to reduction. Thus, the C(2)−C(3) bond was found to be almost (cation **27**) or completely broken (cation **26**).

Summing up, we have tried to calculated the transition state (TS) connecting the bicyclic cation **26** and their "arylium" precursor by means of the quadratic synchronous transit (QST) method.[91] The calculated TS structure has been further checked by the intrinsic reaction coordinate (IRC) approach[92] to verify the TS with respect to studied reaction (see details in Supporting Information). This appeared to connect two equivalent bicyclic structures with only difference in the carbon atom to be attached to the former ipso-carbon C(4). In the structure illustrated in Figure 4 this carbon atom is C(2), and in the equivalent structure this is the C(6) atom (see the Supporting Information). To obtain the potential energy surface profile which does connect the arylium precursor and the final bicyclic structure one should account for the effect of the counterion. This requires more detailed study in further work.

4. CONCLUSIONS

In this paper the global and local electrophilicity indexes for the series of 25 aryl cations in the both singlet and triplet electronic states were studied by means of vertical and adiabatic approximation. Applicability of the latter approach in studying the aryl cations' electrophilicity was proved by comparison of the calculated ω_{adiab} indexes for the cation **4** with the experimental E parameter. The strong dependence between the ω_{adiab} and ω^{+}_{ipso} quantities and the singlet−triplet energy splitting of the aryl cations was found. As expected the ground state cations appeared to be less electrophilic than the excited state species, which is in accordance with the "maximum hardness principle". For the para-methoxyphenyl cation which possesses the isoenergetic singlet and triplet electronic states in MeCN medium, ω_{adiab} = 15.6 eV, and this electrophilicity should be considered as the highest possible for the ground state cations and the lowest for the first excited state one. In the other words the obtained results can be formulated as the following: "the ground state global electrophilicity increases and the first excited state global electrophilicity decreases when the triplet−singlet energy gap goes to zero".

At the same time, the singlet 2,4,6-triamino- and 2,4,6-trimethoxyphenyl cations undergo intramolecular rearrangement when the geometry optimization is completed. This is similar to several ortho-substituted aryl cations studied earlier.[24] The obtained bicyclic cationic structures are characterized by extremely low electrophilicity values ω_{adiab} = 3.16 eV (cation **26**) and ω_{adiab} = 4.54 eV (cation **27**) as well as a strong positive charge delocalization. Furthermore, the ring strain energy values calculated for the 3- and 5-membered rings suggest that these bicyclic cations can exist under the liquid phase conditions. It is worth emphasizing that the mechanism of formation of the cations **26** and **27** requires more detailed study, which will be performed in further papers.

■ ASSOCIATED CONTENT

Supporting Information

Additional information concerning complete reference 65. The static global DFT parameters, QTAIM charges, NICS values, transition structure, and IRC path as well as the statistical analysis concerning the studied aryl cations. This material is available free of charge via the Internet at http://pubs.acs.org.

■ AUTHOR INFORMATION

Corresponding Author

*Fax: (+3) 80472 37-21-42. Tel: (+3) 80472 37-65-76. E-mail: bondchem@cdu.edu.ua.

Notes

The authors declare no competing financial interest.

■ ACKNOWLEDGMENTS

This work was supported by the Ministry of Education and Science of Ukraine, Research Fund (Grant No. 0113U001694). The authors would like to thank Professor Hans Ågren (KTH, Stockholm) for the PDC supercomputer time assignment.

■ REFERENCES

(1) Chattaraj, P. K.; Giri, S.; Duley, S. Update 2 of: Electrophilicity Index. *Chem. Rev.* **2011**, *111*, PR43−PR75.

(2) Chattaraj, P. K.; Giri, S. Electrophilicity Index within a Conceptual DFT Framework. *Annu. Rep. Prog. Chem., Sect. C* **2009**, *105*, 13−39.

(3) Chattaraj, P. K.; Sarkar, U.; Ranjan Roy, D. Electrophilicity Index. *Chem. Rev.* **2006**, *106*, 2065−2091.

(4) Chattaraj, P. K.; Duley, S. Electron Affinity, Electronegativity, and Electrophilicity of Atoms and Ions. *J. Chem. Eng. Data* **2010**, *55*, 1882−1886.

(5) Parr, R. G.; von Szentpály, L.; Liu, S. Electrophilicity Index. *J. Am. Chem. Soc.* **1999**, *121*, 1922−1924.

(6) Domingo, L. R.; Pérez, P. Global and Local Reactivity Indices for Electrophilic/Nucleophilic Free Radicals. *Org. Biomol. Chem.* **2013**, *11*, 4350−4358.

(7) De Vleeschouwer, F.; Van Speybroeck, V.; Waroquier, M.; Geerlings, P.; de Proft, F. Electrophilicity and Nucleophilicity Index for Radicals. *Org. Lett.* **2007**, *9*, 2721−2724.

(8) Domingo, L. R.; Chamorro, E.; Pérez, P. Understanding the Reactivity of Captodative Ethylenes in Polar Cycloaddition Reactions. A Theoretical Study. *J. Org. Chem.* **2008**, *73*, 4615−4624.

(9) Chermette, H. Chemical Reactivity Indexes in Density Functional Theory. *J. Comput. Chem.* **1999**, *20*, 129−154.
(10) Geerlings, P.; de Proft, F.; Langenaeker, W. Conceptual Density Functional Theory. *Chem. Rev.* **2003**, *103*, 1793−1873.
(11) Ess, D. H.; Jones, G. O.; Houk, K. N. Conceptual, Qualitative, and Quantitative Theories of 1,3-Dipolar and Diels−Alder Cycloadditions Used in Synthesis. *Adv. Synth. Catal.* **2006**, *348*, 2337−2361.
(12) Domingo, L. R.; Pérez, P.; Saez, J. A. Understanding the Local Reactivity in Polar Organic Reactions through Electrophilic and Nucleophilic Parr Functions. *RSC Adv.* **2013**, *3*, 1486−1494.
(13) Chattaraj, P. K.; Duleya, S.; Domingo, L. R. Understanding Local Electrophilicity/Nucleophilicity Activation through a Single Reactivity Difference Index. *Org. Biomol. Chem.* **2012**, *10*, 2855−2861.
(14) Domingo, L. R.; Pérez, P. The Nucleophilicity N Index in Organic Chemistry. *Org. Biomol. Chem.* **2011**, *9*, 7168−7175.
(15) Martínez-Araya, J. I.; Salgado-Morán, G.; Glossman-Mitnik, D. Computational Nanochemistry Report on the Oxicams-Conceptual DFT Indices and Chemical Reactivity. *J. Phys. Chem. B* **2013**, *117*, 6339−6351.
(16) Chattaraj, P. K.; Chakraborty, A.; Giri, S. Net Electrophilicity. *J. Phys. Chem. A* **2009**, *113*, 10068−10074.
(17) Parr, R. G.; Donnelly, R. A.; Levy, M.; Palke, W. E. Electronegativity: The Density Functional Viewpoint. *J. Chem. Phys.* **1978**, *68*, 3801−3807.
(18) Parr, R. G.; Pearson, R. G. Absolute Hardness: Companion Parameter to Absolute Electronegativity. *J. Am. Chem. Soc.* **1983**, *105*, 7512−7516.
(19) Laali, K. K.; Rasul, G.; Surya Prakash, G. K.; Olah, G. A. DFT Study of Substituted and Benzannelated Aryl Cations: Substituent Dependency of Singlet/Triplet Ratio. *J. Org. Chem.* **2002**, *67*, 2913−2918.
(20) Aschi, M.; Harvey, J. N. Spin Isomerisation of Para-Substituted Phenyl Cations. *J. Chem. Soc., Perkin Trans. 2* **1999**, 1059−1065.
(21) Harvey, J. N.; Aschi, M.; Schwarz, H.; Koch, W. The Singlet and Triplet States of Phenyl Cation. A Hybrid Approach for Locating Minimum Energy Crossing Points between Non-Interacting Potential Energy Surfaces. *Theor. Chem. Acc.* **1998**, *99*, 95−99.
(22) Lazzaroni, S.; Dondi, D.; Fagnoni, M.; Albini, A. Geometry and Energy of Substituted Phenyl Cations. *J. Org. Chem.* **2008**, *73*, 206−211.
(23) Hrušák, J.; Schröder, D.; Iwata, S. The Ground State ($^1A_1$) and the Lowest Triplet State ($^3B_1$) of the Phenyl Cation $C_6H_5^+$ Revisited. *J. Chem. Phys.* **1997**, *106*, 7541−7549.
(24) Bondarchuk, S. V.; Minaev, B. F. Density Functional Study of Ortho-Substituted Phenyl Cations in Polar Medium and in the Gas Phase. *Chem. Phys.* **2011**, *389*, 68−74.
(25) Protti, S.; Fagnoni, M.; Albini, A. A Photochemical Route to 2-Substituted Benzo[b]furans. *J. Org. Chem.* **2012**, *77*, 6473−6479.
(26) Fagnoni, M.; Dondi, D.; Ravelli, D.; Albini, A. Photocatalysis for the Formation of the C−C Bond. *Chem. Rev.* **2007**, *107*, 2725−2756.
(27) Protti, S.; Dichiarante, V.; Dondi, D.; Fagnoni, M.; Albini, A. Singlet/Triplet Phenyl Cations and Benzyne from the Photodehalogenation of Some Silylated and Stannylated Phenyl Halides. *Chem. Sci.* **2012**, *3*, 1330−1337.
(28) Dichiarante, V.; Fagnoni, M. Aryl Cation Chemistry as an Emerging Versatile Tool for Metal-Free Arylations. *SYNLETT* **2008**, 787−800.
(29) Bondarchuk, S. V.; Minaev, B. F. About Possibility of the Triplet Mechanism of the Meerwein Reaction. *J. Mol. Struct.: THEOCHEM* **2010**, *952*, 1−7.
(30) Minaev, B. F.; Bondarchuk, S. V.; Girţu, M. DFT Study of Electronic Properties, Structure and Spectra of Aryl Diazonium Cations. *J. Mol. Struct.: THEOCHEM* **2009**, *904*, 14−20.
(31) Milanesi, S.; Fagnoni, M.; Albini, A. Cationic Arylation through Photo(Sensitised) Decomposition of Diazonium Salts. Chemoselectivity of Triplet Phenyl Cations. *Chem. Commun.* **2003**, 216−217.
(32) Milanesi, S.; Fagnoni, M.; Albini, A. Sensitized) Photolysis of Diazonium Salts as a Mild General Method for the Generation of Aryl Cations. Chemoselectivity of the Singlet and Triplet 4-Substituted Phenyl Cations. *J. Org. Chem.* **2005**, *70*, 603−610.
(33) Bondarchuk, S. V.; Minaev, B. F.; Fesak, A. Yu. Theoretical Study of the Triplet State Aryl Cations Recombination: A Possible Route to Unusually Stable Doubly Charged Biphenyl Cations. *Int. J. Quantum Chem.* **2013**, *113*, 2580−2588.
(34) Ritchie, C. D. Nucleophilic Reactivities toward Cations. *Acc. Chem. Res.* **1972**, *5*, 348−354.
(35) Pereira, F.; Latino, D. A.; Aires-de-Sousa, J. Estimation of Mayr Electrophilicity with a Quantitative Structure−Property Relationship Approach Using Empirical and DFT Descriptors. *J. Org. Chem.* **2011**, *76*, 9312−9319.
(36) Terrier, F.; Lakhdar, S.; Boubacker, T.; Goumont, R. Ranking the Reactivity of Superelectrophilic Heteroaromatics on the Electrophilicity Scale. *J. Org. Chem.* **2005**, *70*, 6242−6253.
(37) Mayr, H.; Ofial, A. R. Kinetics of Electrophile-Nucleophile Combinations: A General Approach to Polar Organic Reactivity. *Pure Appl. Chem.* **2005**, *77*, 1807−1821.
(38) Mayr, H.; Kempf, B.; Ofial, A. R. π-Nucleophilicity in Carbon−Carbon Bond-Forming Reactions. *Acc. Chem. Res.* **2003**, *36*, 66−77.
(39) Lemek, T.; Mayr, H. Electrophilicity Parameters for Benzylidenemalononitriles. *J. Org. Chem.* **2003**, *68*, 6880−6886.
(40) Mayr, H.; Bug, T.; Gotta, M. F.; Hering, N.; Irrgang, B.; Janker, B.; Kempf, B.; Loos, R.; Ofial, A. R.; Remennikov, G.; et al. Reference Scales for the Characterization of Cationic Electrophiles and Neutral Nucleophiles. *J. Am. Chem. Soc.* **2001**, *123*, 9500−9512.
(41) Mayr, H.; Müller, K. H.; Ofial, A. R.; Bühl, M. H. Comparison of the Electrophilicities of the Free and the (Tricarbonyl)iron-Coordinated Tropylium Ion. *J. Am. Chem. Soc.* **1999**, *121*, 2418−2422.
(42) Arend, M.; Westermann, B.; Risch, N. Modern Variants of the Mannich Reaction. *Angew. Chem., Int. Ed.* **1998**, *37*, 1044−1070.
(43) Mayr, H.; Patz, M. Scales of Nucleophilicity and Electrophilicity: A System for Ordering Polar Organic and Organometallic Reactions. *Angew. Chem., Int. Ed.* **1994**, *33*, 938−957.
(44) Roth, M.; Mayr, H. The Coexistence of the Reactivity−Selectivity Principle and of Linear Free Energy Relationships: A Diffusion Clock for Determining Carbocation Reactivities. *Angew. Chem., Int. Ed.* **1995**, *34*, 2250−2252.
(45) Mayr, H.; Hartnagel, M.; Grimm, R. Quantification of the Electrophilicities of Diazonium Ions. *Liebigs Ann.* **1997**, 55−69.
(46) Schaller, H. F.; Tishkov, A. A.; Feng, X.; Mayr, H. Direct Observation of the Ionization Step in Solvolysis Reactions: Electrophilicity versus Electrofugality of Carbocations. *J. Am. Chem. Soc.* **2008**, *130*, 3012−3025.
(47) Chamorro, E.; Duque-Noreña, M.; Notario, R.; Pérez, P. Intrinsic Relative Scales of Electrophilicity and Nucleophilicity. *J. Phys. Chem. A* **2013**, *117*, 2636−2643.
(48) Denekamp, Ch.; Sandlers, Ya. Electrophilicity−Nucleophilicity Scale Also in the Gas Phase. *Angew. Chem., Int. Ed.* **2006**, *45*, 2093−2096.
(49) Lalli, P. M.; Corilo, Yu. E.; Abdelnur, P. V.; Eberlin, M. N.; Laali, K. K. Intrinsic Acidity and Electrophilicity of Gaseous Propargyl/Allenyl Carbocations. *Org. Biomol. Chem.* **2010**, *8*, 2580−2585.
(50) Dichiarante, V.; Fagnoni, M.; Albini, A. Using Phenyl Cations as Probes for Establishing Electrophilicity−Nucleophilicity Relations. *J. Org. Chem.* **2008**, *73*, 1282−1289.
(51) Pérez, P. Global and Local Electrophilicity Patterns of Diazonium Ions and Their Reactivity toward π-Nucleophiles. *J. Org. Chem.* **2003**, *68*, 5886−5889.
(52) Chattaraj, P. K.; Poddar, A. Molecular Reactivity in the Ground and Excited Electronic States through Density-Dependent Local and Global Reactivity Parameters. *J. Phys. Chem. A* **1999**, *103*, 8691−8699.
(53) Pearson, R. G. The Principle of Maximum Hardness. *Acc. Chem. Res.* **1993**, *26*, 250−255.
(54) Pearson, R. G. Recent Advances in the Concept of Hard and Soft Acids and Bases. *J. Chem. Educ.* **1987**, *64*, 561−570.
(55) Morell, C.; Labet, V.; Grand, A.; Chermette, H. Minimum Electrophilicity Principle: an Analysis Based Upon the Variation of

Both Chemical Potential and Absolute Hardness. *Phys. Chem. Chem. Phys.* **2009**, *11*, 3417−3423.
(56) Chattaraj, P. K.; Giri, S.; Duley, S. Electrophilicity Equalization Principle. *J. Phys. Chem. Lett.* **2010**, *1*, 1064−1067.
(57) Pan, S.; Solà, M.; Chattaraj, P. K. On the Validity of the Maximum Hardness Principle and the Minimum Electrophilicity Principle during Chemical Reactions. *J. Phys. Chem. A* **2013**, *117*, 1843−1852.
(58) Chattaraj, P. K.; Giri, S.; Duley, S. Comment on "Ruling Out Any Electrophilicity Equalization Principle. *J. Phys. Chem. A* **2012**, *116*, 790−791.
(59) von Szentpály, L. Ruling Out Any Electrophilicity Equalization Principle. *J. Phys. Chem. A* **2011**, *115*, 8528−8531.
(60) Kohn, W.; Sham, L. J. Self-Consistent Equations Including Exchange and Correlation Effects. *Phys. Rev. A* **1965**, *140*, A1133−A1138.
(61) Becke, A. D. Density-Functional Thermochemistry. III. The Role of Exact Exchange. *J. Chem. Phys.* **1993**, *98*, 5648−5652, DOI: 10.1063/1.464913.
(62) Lee, C.; Yang, W.; Parr, R. G. Development of the Colle-Salvetti Correlation-Energy Formula into a Functional of the Electron Density. *Phys. Rev. B* **1988**, *37*, 785−789.
(63) Krishnan, R.; Binkley, J. S.; Seeger, R.; Pople, J. A. Self-Consistent Molecular Orbital Methods. XX. A Basis Set for Correlated Wave Functions. *J. Chem. Phys.* **1980**, *72*, 650−654.
(64) Miertuš, S.; Scrocco, E.; Tomasi, J. Electrostatic Interaction of a Solute with a Continuum. A Direct Utilizaion of Ab Initio Molecular Potentials for the Prevision of Solvent Effects. *Chem. Phys.* **1981**, *55*, 117−129.
(65) Frisch, M. J.; Trucks, G. W.; Schlegel, H. B.; Scuseria, G. E.; Robb, M. A.; Cheeseman, J. R.; Scalmani, G.; Barone, V.; Mennucci, B.; Petersson, G. A.; et al. *Gaussian 09, Revision A.02*; Gaussian, Inc.: Wallingford, CT, 2009.
(66) Jensen, F. *Introduction to Computational Chemistry*, 2nd ed.; John Wiley & Sons Ltd: Chichester, 2007.
(67) Parr, R. G.; Yang, W. *Density Functional Theory of Atoms and Molecules*; Oxford University Press: New York, Oxford, 1989.
(68) Delley, B. An All-Electron Numerical Method for Solving the Local Density Functional for Polyatomic Molecules. *J. Chem. Phys.* **1990**, *92*, 508−517.
(69) Delley, B. From Molecules to Solids with the $DMol^3$ Approach. *J. Chem. Phys.* **2000**, *113*, 7756−7764.
(70) *Materials Studio 5.5*; Accelrys, Inc.: San Diego, CA, 2008.
(71) Becke, A. D. A Multicenter Numerical Integration Scheme for Polyatomic Molecules. *J. Chem. Phys.* **1988**, *88*, 2547−2553.
(72) Inada, Y.; Orita, H. Efficiency of Numerical Basis Sets for Predicting the Binding Energies of Hydrogen Bonded Complexes: Evidence of Small Basis Set Superposition Error Compared to Gaussian Basis Sets. *J. Comput. Chem.* **2008**, *29*, 225−232.
(73) Klamt, A.; Schüürmann, G. COSMO: A New Approach to Dielectric Screening in Solvents with Explicit Expressions for the Screening Energy and its Gradient. *J. Chem. Soc., Perkin Trans. 2* **1993**, 799−805.
(74) Delley, B. The Conductor-Like Screening Model for Polymers and Surfaces. *Mol. Simul.* **2006**, *32*, 117−123.
(75) Hirshfeld, F. L. Bonded-Atom Fragments for Describing Molecular Charge Densities. *Theor. Chim. Acta* **1977**, *44*, 129−138.
(76) Van Damme, S.; Bultinck, P.; Fias, S. Electrostatic Potentials from Self-Consistent Hirshfeld Atomic Charges. *J. Chem. Theory Comput.* **2009**, *5*, 334−340.
(77) Fonseca Guerra, C.; Handgraaf, J.-W.; Baerends, E. J.; Bickelhaupt, F. M. Voronoi Deformation Density (VDD) Charges: Assessment of the Mulliken, Bader, Hirshfeld, Weinhold, and VDD Methods for Charge Analysis. *J. Comput. Chem.* **2004**, *25*, 189−210.
(78) de Proft, F.; Van Alsenoy, C.; Peeters, A.; Langenaeker, W.; Geerlings, P. Atomic Charges, Dipole Moments, and Fukui Functions using the Hirshfeld Partitioning of the Electron Density. *J. Comput. Chem.* **2002**, *23*, 1198−1209.
(79) The experimental IE and EA of the methyl, vinyl, and phenyl radicals are available from NIST Chemistry Book Web site.
(80) Domingo, L. R.; Aurell, M. J.; Pérez, P.; Contreras, R. Quantitative Characterization of the Global Electrophilicity Power of Common Diene/Dienophile Pairs in Diels−Alder Reactions. *Tetrahedron* **2002**, *58*, 4417−4423.
(81) Jaramillo, P.; Domingo, L. R.; Chamorro, E.; Pérez, P. A Further Exploration of a Nucleophilicity Index Based on the Gas-Phase Ionization Potentials. *J. Mol. Struct.: THEOCHEM* **2008**, *865*, 68−72.
(82) Ammera, J.; Mayr, H. Photogeneration of Carbocations: Applications in Physical Organic Chemistry and the Design of Suitable Precursors. *J. Phys. Org. Chem.* **2013**, *26*, 956−969.
(83) Mayr, H.; Ofial, A. R. Do General Nucleophilicity Scales Exist? *J. Phys. Org. Chem.* **2008**, *21*, 584−595.
(84) Mella, M.; Coppo, P.; Guizzardi, B.; Fagnoni, M.; Freccero, M.; Albini, A. Photoinduced, Ionic Meerwein Arylation of Olefins. *J. Org. Chem.* **2001**, *66*, 6344−6352.
(85) Morell, Chr.; Grand, A.; Toro-Labbé, A. New Dual Descriptor for Chemical Reactivity. *J. Phys. Chem. A* **2005**, *109*, 205−212.
(86) Tognetti, V.; Morell, Chr.; Ayers, P. W.; Joubert, L.; Chermette, H. A Proposal for an Extended Dual Descriptor: A Possible Solution when Frontier Molecular Orbital Theory Fails. *Phys. Chem. Chem. Phys.* **2013**, *15*, 14465−14475.
(87) Morell, Chr.; Labet, V.; Grand, A.; Ayers, P. W.; de Proft, F.; Geerlings, P.; Chermette, H. Characterization of the Chemical Behavior of the Low Excited States through a Local Chemical Potential. *J. Chem. Theory Comput.* **2009**, *5*, 2274−2283.
(88) Bauzá, A.; Quiñonero, D.; Deyà, P. M.; Frontera, A. Estimating Ring Strain Energies in Small Carbocycles by Means of the Bader's Theory of 'Atoms-in-Molecules'. *Chem. Phys. Lett.* **2012**, *536*, 165−169.
(89) Bader, R. F. W. *Atoms in molecules. A quantum theory*; Clarendon Press: Oxford, 1990.
(90) Keith, T. A. *AIMAll, version 10.07.25*, 2010. http://www.aim.tkgristmill.com.
(91) Peng, Ch.; Schlegel, H. B. Combining Synchronous Transit and Quasi-Newton Methods to Find Transition States. *Isr. J. Chem.* **1993**, *33*, 449−454.
(92) Fukui, K. The Path of Chemical Reactions—The IRC Approach. *Acc. Chem. Res.* **1981**, *14*, 363−368.